The Meteoritical Society

Meteoritics & Planetary Science 42, Nr 2, 155–170 (2007)
Abstract available online at http://meteoritics.org

Olivine-dominated asteroids and meteorites: Distinguishing nebular and igneous histories

Jessica M. SUNSHINE[1*], Schelte J. BUS[2], Catherine M. CORRIGAN[3], Timothy J. McCOY[4], and Thomas H. BURBINE[5]

[1]Department of Astronomy, University of Maryland, College Park, Maryland 20742, USA
[2]University of Hawai'i, Institute for Astronomy, Hilo, Hawai'i 96720, USA
[3]Johns Hopkins University, Applied Physics Laboratory, Laurel, Maryland 20723–6099, USA
[4]Department of Mineral Sciences, National Museum of Natural History, Smithsonian Institution, Washington, D.C. 20560–0119, USA
[5]Department of Astronomy, Mount Holyoke College, South Hadley, Massachusetts 01075, USA
[*]Corresponding author. E-mail: jess@astro.umd.edu

(Received 14 February 2006; revision accepted 19 November 2006)

Abstract–Melting models indicate that the composition and abundance of olivine systematically co-vary and are therefore excellent petrologic indicators. However, heliocentric distance, and thus surface temperature, has a significant effect on the spectra of olivine-rich asteroids. We show that composition and temperature complexly interact spectrally, and must be simultaneously taken into account in order to infer olivine composition accurately. We find that most (7/9) of the olivine-dominated asteroids are magnesian and thus likely sampled mantles differentiated from ordinary chondrite sources (e.g., pallasites). However, two other olivine-rich asteroids (289 Nenetta and 246 Asporina) are found to be more ferroan. Melting models show that partial melting cannot produce olivine-rich residues that are more ferroan than the chondrite precursor from which they formed. Thus, even moderately ferroan olivine must have non-ordinary chondrite origins, and therefore likely originate from oxidized R chondrites or melts thereof, which reflect variations in nebular composition within the asteroid belt. This is consistent with the meteoritic record in which R chondrites and brachinites are rare relative to pallasites.

INTRODUCTION

Olivine has long held a special role for its utility in understanding the origin and evolution of meteorites and, by extension, the asteroids from which they originate. As the dominant mineral in most chondritic meteorites, early researchers easily separated olivine, and olivine composition was among the earliest criteria for classifying meteorites (e.g., Mason 1963). A key characteristic of olivine is that its abundance and composition co-vary in predictable fashion as a result of both nebular and igneous processes. Thus, olivine abundance and composition can serve as a unique fingerprint of the processes that formed a meteorite or an asteroid. While meteoriticists have exploited the abundance and composition as markers of petrogenesis for decades, a paucity of quality spectral data has prevented spectroscopists from confidently using the same approach to remotely explore asteroids. This is particularly true for the olivine-rich asteroids, which have remained few in number and poorly studied. In this paper, we show that simultaneous solution of both olivine abundance and composition, demonstrated on high-quality meteorite and asteroid spectra, can be used to infer the origin of olivine-rich asteroids.

Chondritic Olivine

Olivine is the dominant mineral in ordinary, carbonaceous, and the highly oxidized R chondrites, but also can be found at the few volume percent level even in the least-metamorphosed members of the highly reduced enstatite chondrites (Brearley and Jones 1998). Within and between these groups, a gross relationship between olivine to pyroxene ratios and olivine composition is observed, with the most olivine-rich chondrites (e.g., R, LL chondrites) having the most ferroan olivine and least olivine-rich chondrites (e.g., H, E chondrites) having the most magnesian olivine. These broad differences likely reflect the oxidation state of the region of the nebula in which each group formed, although differences in bulk and oxygen isotopic composition preclude a simple oxidation-reduction relationship (Rubin et al. 1988).

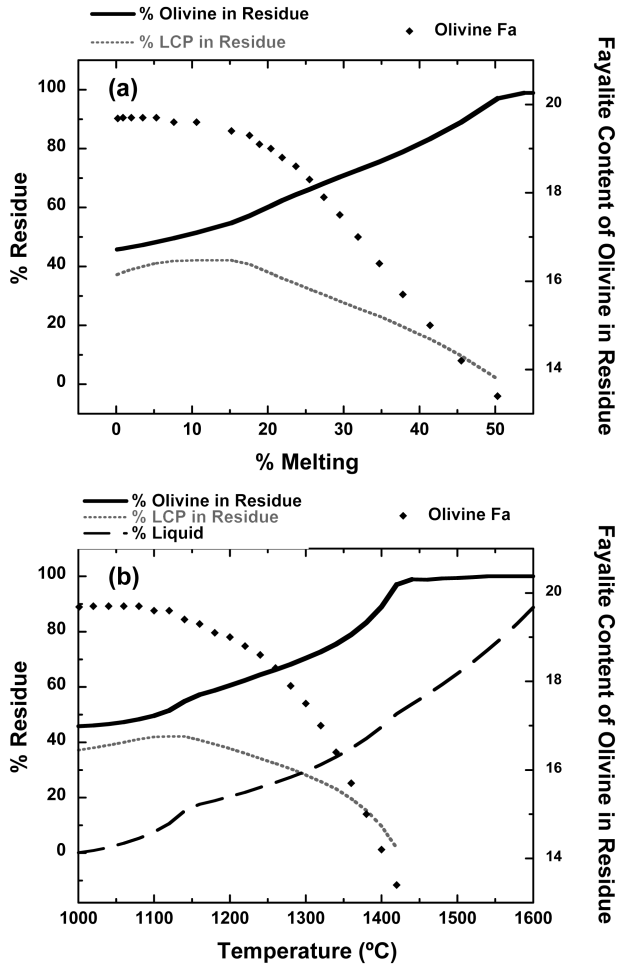

Fig. 1. H chondrite melting. Olivine and low-calcium pyroxene abundances and olivine composition (Fa) in the residue calculated using the MELTS program (Ghiorso and Sack 1995; Asimow and Ghiorso 1998) from melting of an H chondrite at fO_2 of IW and calculated at 20 °C temperature intervals. Pallasites with olivine ($Fa_{10–12}$) ± minor low-calcium pyroxene ($Fs_{10–12}$) can be produced (a) as residues of ~45–70% partial melting and (b) at temperatures of ~1400–1500 °C.

The correlation of olivine-rich and ferroan compositions suggests that nebular oxidation is incapable of producing an olivine-rich chondrite with magnesian composition. The trend in olivine abundance and composition is also apparent within the ordinary chondrites which progress from H chondrites (35% olivine, 26% low-calcium pyroxene, olivine composition Fa_{18}) (Gomes and Keil 1980; McSween et al. 1991) to LL chondrites (52% olivine, 21% low-calcium pyroxene, olivine composition Fa_{28}) (Gomes and Keil 1980; McSween et al. 1991).

Differentiated Chondrites

While chondritic meteorites show that increasing FeO in olivine is correlated with increasing olivine abundance, differentiation produces essentially the opposite trend. Partial melting of a chondrite produces early silicate partial melts (following melting of the Fe, Ni-FeS cotectic) that are enriched in plagioclase and pyroxene and are markedly more ferroan than the residue. Thus, the residue becomes increasingly olivine-rich and magnesian with increased partial melting. This is shown in Fig. 1, which illustrates the percent of olivine and low-calcium pyroxene and the composition of olivine in the residue produced during melting of an average H chondrite as calculated using the MELTS program at an fO_2 of IW (Asimow and Ghiorso 1998; Ghiorso and Sack 1995). We chose a starting silicate composition as input into the MELTS program based on a re-normalization of the H chondrite composition from Jarosewich (1990) after removal of the metal and sulfide components. The percentage of olivine in the residue increases steadily until it reaches pure olivine at 1540 °C. At the same time, the olivine composition decreases steadily from $Fa_{19.7}$ (1000 °C) to $Fa_{6.4}$ (1620 °C). Low-calcium pyroxene abundances in the residue increase slightly as plagioclase and clinopyroxene melt and then decrease steadily until completely melted at ~1440 °C. The percent of melt increases steadily with temperature, exhibiting inflections at the points where high-calcium pyroxene and low-calcium pyroxene are exhausted from the residue. These results show that lithologies with olivine ($Fa_{10–12}$) ± minor low-calcium pyroxene ($Fs_{10–12}$), for example pallasites, can be produced as residues of ~45–70% partial melting at temperatures of ~1400–1500 °C.

These calculations demonstrate that mantle material formed as a residue of partial melting of ordinary chondritic material is expected to be olivine-rich and that the olivine should exhibit magnesian composition. Thus, the conventional wisdom that pure olivine lithologies with magnesian olivine compositions are produced only during differentiation is probably correct. Our melt modeling shows that such compositions form during differentiation, while, as discussed below, nebular processes producing olivine-rich compositions yield much more ferroan olivine. Yet, owing in part to data inadequate to examine both olivine abundance and composition, asteroid spectroscopists have commonly assumed that identification of a pure olivine assemblage alone—in the absence of information about the composition of that olivine—is sufficient evidence of a mantle origin.

The origin of other olivine-rich asteroids from examining the MELTS modeling is less clear. For example, highly differentiated mantles need not exclude pyroxene. Our calculations suggest that in a narrow temperature range near ~1400–1420 °C and partial melting of ~45–50%, we can produce an olivine-rich lithology with minor (2–10%) low-calcium pyroxene with both olivine and low-calcium pyroxene compositions that match those of pyroxene-bearing pallasites. The recognition of pyroxene pallasites (Boesenberg et al. 2000) suggests not all asteroids melted to the point that produces olivine-only residues, perhaps having

been limited by heat sources and/or heat loss by convective processes (McCoy et al., Forthcoming).

A more intriguing (and ambiguous) case exists for an olivine-rich asteroid with more ferroan (e.g., $Fa_{\sim 40}$) olivine composition. Nebular processes can produce such a composition, and the highly oxidized R chondrites are an example (Schulze et al. 1994). These meteorites tend to be olivine-rich with olivine to pyroxene ratios ranging from 11:1 to 6:1. The type meteorite, Rumuruti, contains 70.4 vol% olivine, 0.5 vol% low-calcium pyroxene and 5.2 vol% clinopyroxene. Compositionally, olivine ranges from $Fa_{0.4\text{-}42.6}$, but the vast majority of grains are ferroan ($Fa_{37.0\text{-}42.6}$). Although some differences exist between individual R chondrites, they are as a group olivine-rich and ferroan, with minor amounts of co-existing high-calcium pyroxene.

It also appears that igneous processes can produce olivine-rich, ferroan compositions (Mittlefehldt et al. 2003). The igneous-textured brachinites—only recognized as a distinct group within the last decade—typically contain 80–90% olivine, 5–10% clinopyroxene and a trace of low-calcium pyroxene. Olivine has a composition of $Fa_{\sim 35}$. Metamorphism and melting in the presence of an oxidizing agent (converting magnesian pyroxene and metal to ferroan olivine) has been invoked for the brachinites (Nehru et al. 1996). It is also possible that brachinites are residues of the melting of a more ferroan chondrite. Figure 2 illustrates the residue produced by melting of the silicate fraction of the R chondrite Rumuruti (Jarosewich, personal communication), demonstrating both similarities and differences to melting of a reduced chondritic precursor such as H chondrites (Fig. 1). These calculations were performed using the MELTS model (Asimow and Ghiorso 1998; Ghiorso and Sack 1995) at an fO_2 of QFM, since both R chondrites and brachinites appear to record more oxidizing conditions. As in the earlier case, olivine abundances increase and Fa concentrations decrease with increasing temperature and partial melting. In this case, only high-calcium pyroxene is observed and it is exhausted from the residue by 1120 °C. It is interesting to note that a nearly pure olivine residue (98.5% olivine) with olivine of $Fa_{\sim 35}$ is produced at ~25% melting and a temperature of 1220 °C, although this residue lacks the clinopyroxene observed in brachinites. Our calculations show that partial melting cannot produce olivine that is more ferroan than the chondritic precursor from which it formed and, thus, cannot be invoked to explain either Fa-rich (e.g., Fa_{60}), olivine-rich asteroids (Reddy et al. 2005) or inferred olivine compositions more fayalitic than ordinary chondrites on S-asteroids (McFadden et al. 2005).

Clearly, it would be difficult to distinguish whether an olivine-rich asteroid with moderately ferroan olivine was an oxidized chondrite or the product of low-degrees of partial melting of such a chondrite, particularly given the uncertainties in olivine abundance and composition derived from spectral data. Two features that might distinguish these

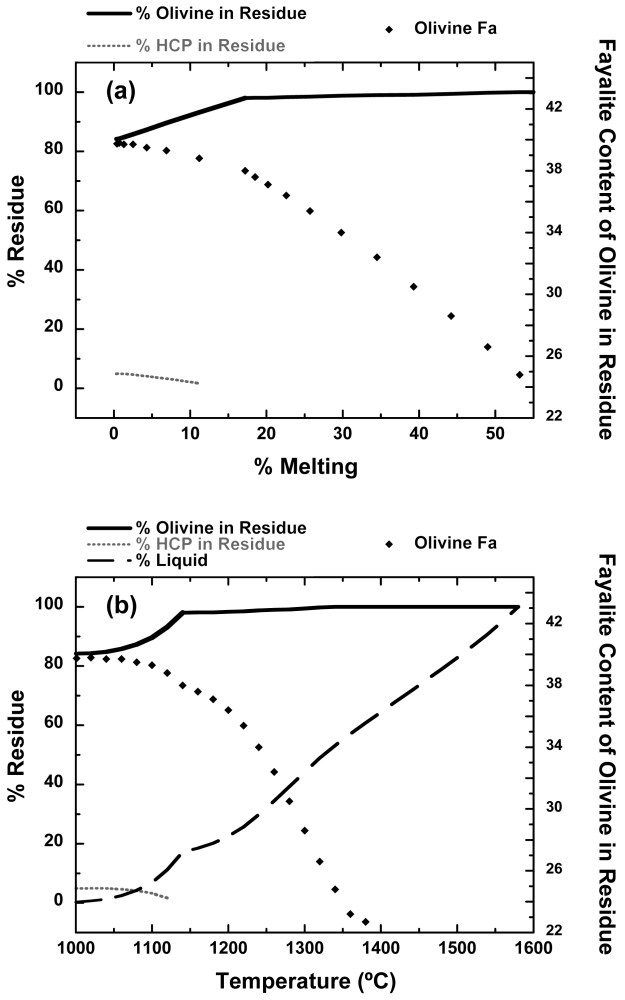

Fig. 2. R chondrite melting. Olivine and low-calcium pyroxene abundances and olivine composition (Fa) in the residue calculated using the MELTS program (Ghiorso and Sack 1995; Asimow and Ghiorso 1998) from melting of the R chondrite Rumuruti at fO_2 of QFM and calculated at 20 °C temperature intervals. Melting of an R chondrite can produce olivine-rich residues with Fa concentrations appropriate to brachinites (a) at ~25% melting and (b) a temperature of ~1220 °C.

groups of meteorites are the extent of the lithologies and what other materials might be expected to co-exist. While R chondrites probably represent a lithology present on an asteroidal scale, it is unknown if brachinites can occur on the global scale (e.g., by asteroid differentiation and formation of a brachinite mantle) or are only formed on a local scale (e.g., within a smaller magma chamber) (Mittlefehldt et al. 2003). Some features of the brachinites point to differences in degree of oxidation and igneous fractionation and may have derived from distinct, and thus local, magmas. In addition, the brachinites must have had a complementary basaltic component at some point in their history. If derived from local magma chambers, some of this basaltic component might be expected to have survived on the brachinite parent body.

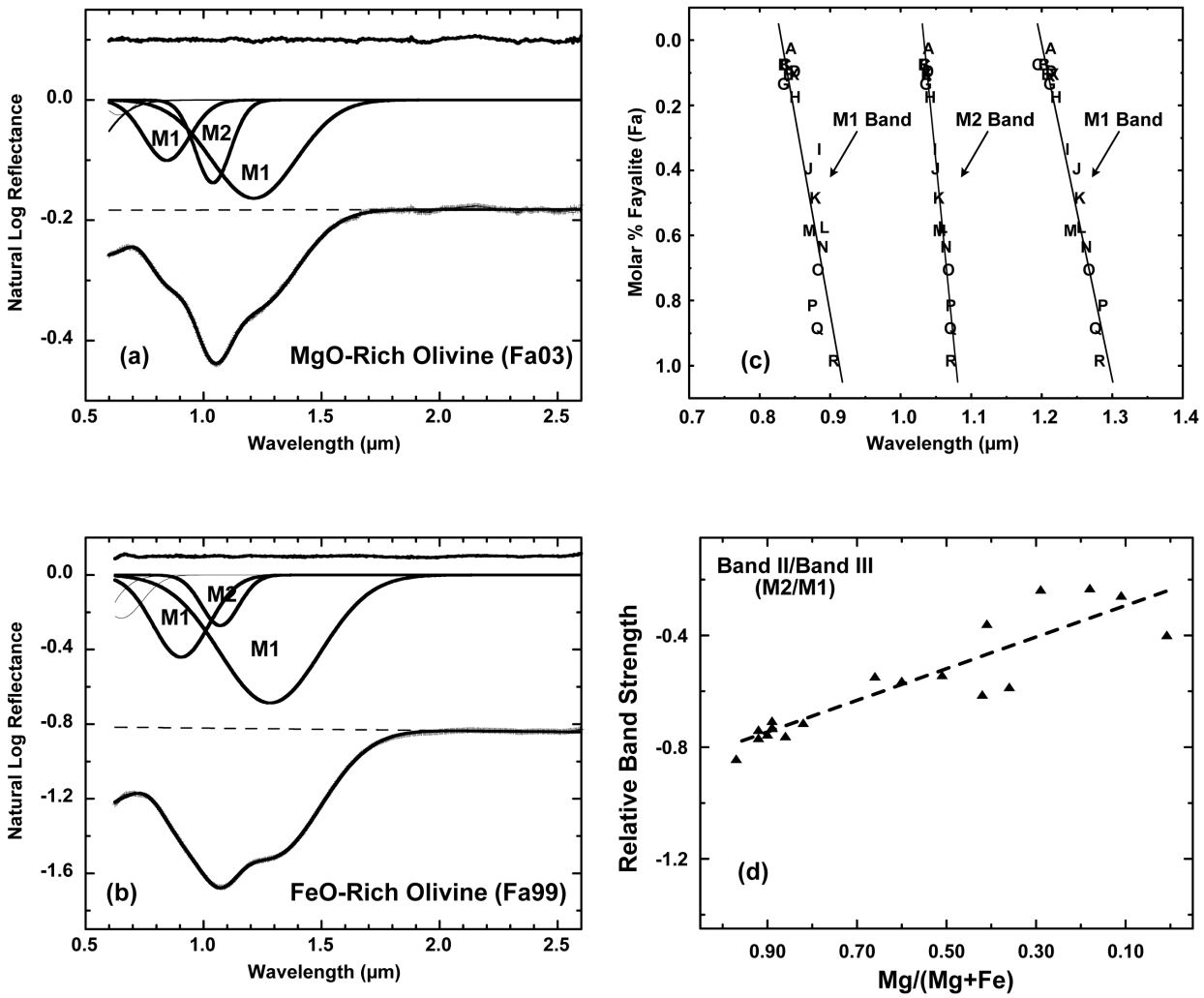

Fig. 3. Olivine absorptions as a function of composition. MGM fits to (a) Fa_{03} and (b) Fa_{99} showing differences in relative strengths and positions of major absorptions (bold) from the M1 and M2 crystallographic sites. Additional minor absorptions at shorter wavelengths are also included in the model as thin lines. Trends across a complete range of compositions of olivine spectra are shown for (c) band centers and (d) relative strengths of the M2/M1 bands. Under the MGM, the measured spectrum is model as a sum of modified Gaussian distributions superimposed onto a baseline (dashed line). The residual error between the data and the fit is shown at the top, offset 10% for clarity. These trends can be used to constrain models and to infer composition of olivine from their spectra. Modified from Sunshine and Pieters (1998).

It is clear that olivine can act as a tracer of the history of a specific meteorite or asteroid, although reading that history requires knowledge of both the abundance and composition of olivine and the controlling processes. It is equally clear that the search for the elusive asteroidal mantles is not as simple as identifying an asteroid as olivine-rich. Indeed, some olivine-rich asteroids, those that are more ferroan, may sample processes of nebular oxidation or partial melting thereof only uncovered in the meteorite record within the last decade.

BACKGROUND

Spectrally, olivine is characterized by a dominant, complex, absorption feature near 1 μm arising from electronic transitions of Fe^{+2}, which occupies both the M1 and M2 crystallographic sites (e.g., Figs. 3a and 3b). These distorted octahedral sites lead to three distinct, but overlapping, absorption bands in the 1 μm region. The overall 1 μm feature is known to change with iron content across the fayalite-forsterite (ferroan-magnesian) solid solution series, which can be used to infer composition (Burns 1970, 1993; King and Ridley 1987). In addition, as discussed below, Sunshine and Pieters (1998) showed that the position and relative strengths of the individual bands that comprise the 1 μm absorption feature in olivine spectra vary systematically with composition, which together can be used to confidently infer olivine composition from reflectance spectra. However, as discussed in detail below, temperature effects are significant in olivine spectra and must be taken into account when inferring composition from reflectance spectra of planetary surfaces.

Absorption Band Modeling of Olivine Spectra

The three individual absorption bands that comprise the dominant 1 μm feature in olivine spectra can be resolved by modeling. In particular, Sunshine et al. (1990) developed an absorption band model based on a physical understanding of crystal field absorptions. This Modified Gaussian Model (MGM) has been shown to accurately model the shape of isolated crystal field absorptions and thereby provides a high degree of confidence in resolving overlapping absorption bands (e.g., Hiroi and Sasaki 2001; Mustard 1992; Schade and Wäsch 1999; Sunshine and Pieters 1993, 1998; Ueda et al. 2003). Under the MGM, spectra are modeled in apparent absorbance (log reflectance invoking Beer's law) and energy, as a series of modified Gaussian distributions superimposed onto a baseline continuum. Each absorption band is described by three model parameters: band center, width, and strength. The continuum is a straight line in energy and is described by two additional parameters, a slope and an offset. Unlike traditional continuum removal techniques (e.g., Cloutis et al. 1986; McCord et al. 1981), the MGM continuum is not forced to be tangent to the spectrum, but rather is optimized along with other model parameters in the fitting process. This allows for overlap between absorption bands that may produce apparent absorption maxima.

Using the MGM, Sunshine and Pieters (1998) quantified variations in the position and relative strength of individual absorption bands in the 1 μm olivine feature as a function of composition. Absorptions at shorter wavelengths are also included in the modeling, but were not found to be systematically related to Fe/Mg composition. However, each of the individual absorption bands (two M1 and one M2) was found to move systematically towards longer wavelengths as the composition becomes more ferroan (see Figs. 3a and 3b). The positions of these major bands can be retrieved with the MGM and can thereby be used to infer Fe/Mg concentration. In these laboratory spectra, the fayalite content resulting from MGM analyses has 5% errors (see Fig. 3c). Equally important, the relative strength of the M1 versus M2 absorptions also systematically varies as a function of composition, with the ratio of M2 to M1 band strengths increasing as the composition becomes more magnesian (see Fig. 3d).

Previous Analyses of Olivine-Rich Asteroid Spectra

One of the long standing issues in our current understanding of the makeup of the asteroid belt is the paucity of olivine-dominated metal-free silicate objects both in the Main Belt and in meteorite collections (Bell et al. 1989; Chapman 1986). It has been proposed (Burbine et al. 1996) that the rarity of such olivine-dominated (metal-free) and basaltic asteroids is caused by the fact that all or most of the differentiated asteroids have been broken down during collisions, possibly disengaging mantle and crustal material from core material. Since asteroidal core material (Fe,Ni metal) is more resistant to destruction than silicate crustal material, it is reasonable to expect the oldest material delivered to Earth to represent core material (iron meteorites) and possibly mantle material (pallasites). An additional complication in recognizing metal-free olivine asteroids spectrally could be space weathering, which optically alters the surfaces of asteroids (Clark et al. 2003; Pieters et al. 1993; 2000; Wetherill and Chapman 1988).

Taxonomic classifications of asteroid spectra have lead to the categorization of A-asteroids, which, while defined spectrally, have become synonymous with olivine-rich materials, even though olivine-dominated assemblages are known to exist in the S-asteroid population (Gaffey et al. 1993). A-asteroids are relatively rare, with only about 20 A-asteroids identified from visible spectra (Bus and Binzel 2002a). However, as discussed below only seven have near-IR spectra that are dominated by olivine absorptions. On the other hand, two additional objects originally classified as S-asteroids are spectrally dominated by olivine absorption bands. The A-asteroid class was first proposed by Veeder et al. (1982, 1983) using near infrared (1.0–2.2 μm) observations of asteroids 446 Aeternitas and 863 Benkoela that were seen to exhibit red J-H colors. Based on these two asteroids, Veeder et al. (1983) proposed that these asteroids have an olivine-rich surface composition and that A-asteroids are an extension of a spectral trend from pyroxene- to olivine-rich surfaces, i.e., from Vesta (and the V-type asteroids) to R- to S-, and finally to A-type asteroids. Tholen (1984) further refined the A-class with data from the visible Eight-Color Asteroid Survey (ECAS) data. Subsequently, Bus and Binzel (2002b) used their visible CCD spectra to place objects in the A asteroid group.

The first complete near infrared (0.8–2.6 μm) spectral observations of A-asteroids were carried out by Cruikshank and Hartmann (1984). They observed asteroids 246 Asporina and 289 Nenetta and detected the characteristic 1 μm absorption feature indicative of olivine. The lack of other mafic absorptions suggested <10% pyroxene and/or plagioclase feldspar. Based on simple spectral matching with existing laboratory data, Cruikshank and Hartmann inferred that both asteroids have forsteritic surface compositions (Asporina $Fa_{10–40}$ and Nenetta $Fa_{20–60}$), are composed of pulverized material, and possibly contain a large fraction of metal. The only known olivine-rich meteorites, Chassigny, Brachina, and pallasites, were offered as plausible analogs to these olivine asteroids. However, a Chassigny link was ruled out based on its Martian origin.

Other workers (Bell et al. 1984a, 1984b; Cloutis et al. 1990) analyzed the spectrum of 446 Aeternitas and hypothesized a surface mineralogy that is a mixture ~35–60% metallic iron (indicated by the redder continuum slope from 0.7–1.5 μm), ~40–55% olivine, and ~10% pyroxene. Cloutis et al. (1990) suggested that the olivine composition of

446 Aeternitas appears to be $Fa_{20 \pm 10}$ (presumably from spectral matching with laboratory samples). Based on the inferred metal to olivine ratio and olivine composition, Cloutis et al. (1990) concluded that 446 Aeternitas is most similar to Eagle Station pallasites, possibly indicating a parental relationship. However, they note that these pallasites have less pyroxene than 446 Aeternitas. Interestingly, rather than a significant amount of metal, Bell et al. (1984b) offered that 446 Aeternitas could be fayalitic. Yet, they prefer a metallic and forsteritic interpretation, and therefore suggest a link to pallasite meteorites.

Gaffey (1998) suggested that an absorption band near 0.65 μm in olivine spectra could be used as a tracer for oxidation history based on a link to nickel content (King and Ridley 1987). However, Sunshine and Pieters (1998), analyzing a larger range of olivine spectra, questioned the association of this absorption with nickel. Instead, they determined that the feature is dependent on particle size and is enhanced in small particles. In addition, comparing particle spectra <45 μm, Sunshine and Pieters (1998) found that the 0.65 μm absorption band is only present in the spectra of ferroan (>Fa_{44}) olivines and therefore linked to iron charge transfer and/or electronic transition absorptions. Assuming that the 0.65 μm absorption is due to olivine and not some minor phase present in all the laboratory FeO-rich olivines (e.g., opaque), Sunshine et al. (1998) used this result to suggest that spectra of olivine-rich asteroids that contain a 0.65 μm feature in visible telescopic spectra may be ferroan.

Using data from 0.90–1.65 μm, Burbine and Binzel (2002) subdivided the A-asteroids into two groups based on the strength of their spectral features. They found that A-asteroids with diameters of ~10 km had much weaker 1 μm absorption bands than larger A-asteroids. This is contrary to the trend one would expect from any space weathering effects in which smaller, presumably younger, asteroids would be less weathered and therefore have stronger 1 μm absorptions. Thus, the weaker 1 μm absorptions were used to argue for diversity in composition, likely metal abundance, among the A-asteroids.

For the first time, the effects of temperature on interpreting olivine-rich asteroid spectra were taken into consideration by Lucey et al. (1998). They proposed that the systematic differences they observed in the width of the olivine absorption feature in A-asteroid spectra compared to magnesian olivine spectra obtained in laboratory measurements could be due to the low temperatures on the surfaces of bodies in the Main Belt versus room temperature. They compared spectra of forsteritic olivine obtained at low temperatures (Roush and Singer 1987; Singer and Roush 1985) and found better matches to the asteroid spectra. Furthermore, they attempted to extrapolate the effects of temperature to higher iron olivine compositions and thereby ruled out low-temperature ferroan olivines without any actual spectra of such compositions at lower temperatures. After accounting for temperature effects, Lucey et al. (1998) therefore concluded that the compositions of all the A-asteroid surfaces they considered (246 Asporina, 289 Nenetta, 446 Aeternitas, and 863 Benkoela) are olivine ~Fa_{10}, further strengthening the conventional wisdom that the A-asteroids are the parent bodies of the pallasites.

Reddy et al. (2005) further explored the effects of temperature on olivine-rich asteroid spectra. They examined 246 Asporina, 289 Nenetta, and 446 Aeternitas at different heliocentric distance and thus different average surface temperatures. However, over the very limited range of observed temperatures, less than 10 K, no changes in absorption characteristics were identified. Using the position of the overall 1 μm absorption feature and the laboratory work of King and Ridley (1987), they concluded that 446 Aeternitas and 246 Asporina have olivine compositions of $Fa_{30 \pm 20}$ and $Fa_{60 \pm 20}$, respectively. However, no petrologic interpretations or meteoritic links were offered.

Sunshine and Pieters (1998) and Sunshine et al. (1998) extended their MGM modeling of laboratory spectra of various compositions of olivine to existing spectra of A-asteroids. Sunshine and Pieters (1998) showed that unconstrained modeling of asteroid spectra resulted in solutions that were inconsistent with the variations observed in olivine spectra in the laboratory, and thus the results were deemed physically unrealistic. Instead, a method using the systematic compositional variations in both the relative band strengths and the position of absorptions in olivine was developed and tested. Endmember models with relative strengths typical of MgO-rich olivines (i.e., relatively strong M2/M1 bands; see Fig. 3d) or FeO-rich olivines (i.e., relatively weak M2/M1 bands) and correlated band centers are tested against the measured spectrum, and the results are then evaluated for consistency. For example, when these constrained models were applied to the 52-color spectrum of 246 Asporina (Bell et al. 1984b) they indicated that the olivine on the surface of the A-asteroid 246 Asporina is magnesian (>Fa_{20}), as models with relative band strengths typical of more ferroan olivine were inconsistent in that they required band centers at wavelengths that imply magnesian compositions. A similar analysis of 52-color data of 863 Benkoela also suggested a magnesian olivine composition (<Fa_{15}) (Sunshine et al. 1998). However, using the same approach but with newer data from the SMASSIR survey (Burbine and Binzel 2002), Sunshine et al. (1998) suggested that 289 Nenetta was more ferroan with a composition of ~Fa_{30}, and thus could be petrologically related to the brachinite meteorites. However, neither of these studies took into account the effects of temperatures in the Main Belt.

In order to characterize the surface of the A-asteroid 1951 Lick, de León et al. (2004) also used the MGM to model spectra collected in the visible with the 2.5 m Nordic Optical Telescope (NOT) equipped with the Andalucia Faint Object Spectrograph and Camera (ALFOSC), and in the near-

infrared using the Near-Infrared Camera Spectrograph (NICS) on the Telescopio Nazionale Galileo (TNG). They first used measurements of the overall position, area, and slope of absorption features in 1951 Lick compared to those of a laboratory measurement of the spectrum of Brachina (Fa_{66}). They found excellent agreement, both visually and in all band parameters (except slope), between 1951 Lick and Brachina. However, when the constrained MGM modeling approach defined by Sunshine and Pieters (1998) was employed, de León et al. found that the individual band centers and relative strengths of 1951 Lick are most consistent with olivine compositions of $Fa_{10 \pm 10}$.

Using data available at the time of their analyses, numerous researchers have attempted to determine the composition of olivine on the surfaces of asteroids. A summary of the previous studies discussed above shows significant differences among the olivine compositions derived by different workers (Table 1). The possibility that such compositional information could be used to establish potential links to pallasites or to brachinites dates back to the work of Cruikshank and Hartmann (1984). However, since then, the majority of researchers have neglected (often simply dismissing) the brachinites and largely concluded that all A-asteroids are the parent bodies of pallasites. These conclusions were based in part on the fact that previous asteroid spectra had only enough spectral resolution and signal-to-noise to support the identification of a strong 1 μm absorption feature, and lacked enough detail to confidently infer composition. In addition, these previous researchers often neglected the effects of temperature on spectra of Main Belt A-asteroids.

Recent advances in instrumentation have led to significant improvements in the quality and spectral range of asteroid spectra. This new generation of data can support more detailed and quantitative analysis than was possible in the past (e.g., Sunshine et al. 2004), including confidently inferring the compositions of olivine on A-asteroids from their spectra. In this work, we analyze near-infrared data obtained at the NASA Infrared Telescope Facility (IRTF) on Mauna Kea with SpeX, a low- to medium-resolution near-infrared spectrograph, which in low-resolution mode collects data from 0.8 to 2.5 μm in a single observation, with a spectral resolution of R ~100 (Rayner et al. 2003). We also re-examine the spectrum of 1951 Lick collected by de Leon et al. (2004). In addition, our MGM-based modeling techniques now simultaneously include the effects of both temperature and composition.

To test our analysis methods and the relevance of our results, we first use the MGM to examine laboratory spectra of well-characterized olivine-rich meteorites. We present and analyze the spectra of the broader range of meteorites currently available in our collections including R chondrites, new brachinites, and unweathered olivine collected from a pallasite. Finally, we present compositional and petrologic inferences for three Main Belt and one near-Earth olivine-dominated asteroids. Five other olivine-rich spectra were measured by SpeX, which in addition to strong 1 μm olivine-absorptions features have absorptions in the 2 μm region and therefore clearly include pyroxenes. Detailed modeling of combinations of pyroxenes and olivines is nontrivial (see Sunshine 1995) and beyond the scope of this work. However, the melt modeling presented earlier (Figs. 1 and 2) indicates that the composition of the co-existing pyroxene (high- or low-calcium) provides an additional constraint on petrologic origin.

Table 1. Summary of previous compositional inferences for olivine-dominated asteroids.

Asteroid	Inferred olivine composition	Researcher
246 Asporina	$Fa_{10–40}$	Cruikshank and Hartmann (1984)
	$<Fa_{5–15}$	Lucey et al. (1998)
	$<Fa_{20}$	Sunshine et al. (1998)
	$Fa_{40–80}$	Reddy et al. (2005)
289 Nenetta	$Fa_{20–60}$	Cruikshank and Hartmann (1984)
	$<Fa_{5–15}$	Lucey et al. (1998)
	$\sim Fa_{40}$	Sunshine et al. (1998)
446 Aeternitas	$Fa_{10–20}$	Cloutis et al. (1990)
	Forsteritic	Bell et al. (1984b)
	If no metal, could also be ferroan	Bell et al. (1984b)
	$<Fa_{5–15}$	Lucey et al. (1998)
	$Fa_{10–50}$	Reddy et al. (2005)
863 Benkoela	$<Fa_{5–15}$	Lucey et al. (1998)
	$<Fa_{15}$	Sunshine et al. (1998)
1951 Lick	$Fa_{0–20}$	de León et al. (2004)

OLIVINE-RICH METEORITES

Sample Descriptions

In order to establish a baseline for comparison to asteroids and to test our analysis techniques on samples with known composition, we collected samples and spectra of three olivine-rich meteorites that span the range of olivine compositions. Preliminary results of this research were presented by Sunshine et al. (2005).

Pallasites have been widely cited as the best meteoritic analog for A-asteroids, but relatively few high-quality spectra of unweathered olivine from pallasites exist. We separated ~200 mg of minimally weathered, loose olivine fragments from the Thiel Mountain pallasite (USNM 6356). Thiel Mountain is a typical main-group pallasite with subequal mixture of Fe,Ni metal and magnesian olivine of composition Fa_{13}. The olivine grains were selected from a vial of material liberated during cutting and that included grains ranging from highly to minimally weathered. We handpicked grains that exhibited minimal staining and during repeated crushing removed fragments that exhibited any staining or inclusions.

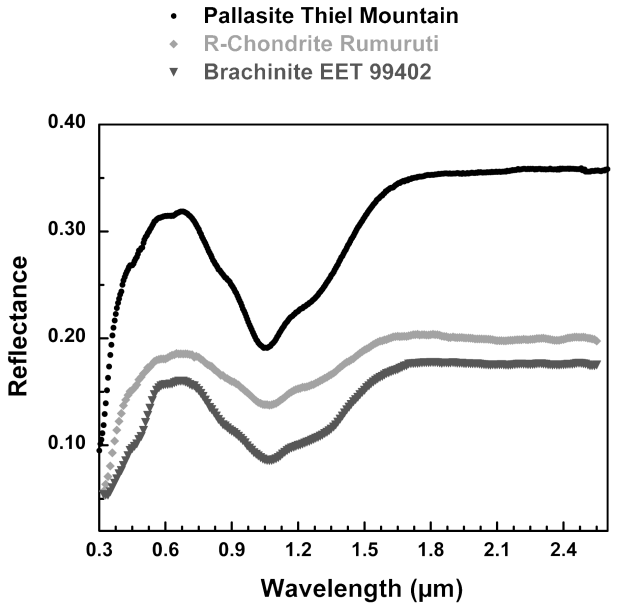

Fig. 4. Spectra of representative olivine-dominated meteorite classes.

Rumuruti is the type specimen of the R chondrites, a group of highly oxidized chondrites, and the only observed fall from the group. Rumuruti is rich in olivine (~70 vol% olivine) and contains high-calcium pyroxene (~5 vol%)—the only other abundant mafic silicate (with minor amounts of low-calcium pyroxene and feldspar, and trace amounts of chromite, phosphate, metal, and troilite). The olivine compositions in Rumuruti exhibit a broad range ($Fa_{1–42}$), but with most grains around Fa_{39} (Schulze et al. 1994). We examined materials crushed from the bulk meteorite (USNM 6826) as described by Burbine et al. (2003).

Finally, we analyzed a sample of the EET 99402 brachinite. EET 99402 is typical of brachinites in that it contains abundant olivine (~86 vol%) with high-calcium pyroxene (~5 vol%) as the only other abundant mafic silicate (with minor to trace low-calcium pyroxene, plagioclase, metal, troilite, chromite, and phosphate). The olivine in EET 99402 is moderately ferroan, Fa_{36} (Mittlefehldt et al. 2003). It should be noted that, based on mafic silicate abundances and compositions, there is little to distinguish R chondrites from brachinites.

Composition of Olivine-Dominated Meteorites: Testing the MGM

To build confidence in our results and to provide a basis for comparison to asteroid spectra, we first used the MGM to examine the spectra of clean, well-characterized samples from the three major groups of olivine-dominated meteorites, as described above. Reflectance spectra of these samples are shown in Fig. 4. These reflectance spectra were obtained using the bi-directional spectrometer at Brown University's Keck/NASA Reflectance Experiment Laboratory (RELAB; Pieters and Hiroi 2004). Specific details of these three samples and their spectra are given in Table 2.

All three meteorite spectra are dominated by a complex absorption feature centered near 1 μm. The spectrum of Rumuruti also includes of weak absorption near 2 μm, indicating the presence of minor amounts of pyroxene, which in turn required the addition of a corresponding pyroxene band in the 1 μm in the fit. None have significant absorptions due to alteration products, attesting to their purity. These spectra were modeled with the MGM to determine if the olivine compositions derived from the results are consistent with their known chemistry. MGM fits to the three meteorite spectra shown in Fig. 5.

As described by Sunshine and Pieters (1998), the position of the three olivine bands can be used to infer olivine composition with accuracy in the laboratory of ±5%. Band centers from MGM modeling of Thiel Mountain pallasite imply a composition of ~Fa_{10}, while EET 99402 and Rumuruti are more ferroan, ~Fa_{30} and ~Fa_{35}, respectively. In all cases, the inferred compositions are within the ±5% uncertainties when compared to geochemical data (Fa_{13}, Fa_{36}, and Fa_{39}, respectively). Given the excellent agreement between olivine compositions derived from MGM modeling and known compositions, it is clear the spectroscopy provides reliable information on olivine composition. These results build confidence in using MGM analyses of spectra of olivine-rich asteroids and other olivine-rich surfaces to infer their petrologic origin.

VARIATIONS IN OLIVINE SPECTRA WITH TEMPERATURE

As noted by Lucey et al. (1998), extension of these results to analyses of asteroid spectra adds a level of complexity due to the surface temperature of asteroids. To a first order, two groups exist: the Main Belt population, which has surface temperatures near 170 to 190 K, and the near-Earth asteroids with temperatures near 250 to 300 K, similar to standard laboratory conditions. Singer and Roush (Roush and Singer 1987; Singer and Roush 1985) showed that significant variations in olivine reflectance spectra with temperature exist for the range of surface temperatures possible among the asteroid population. In particular, the olivine absorption feature narrows with decreasing temperature. New measurements and analyses (Hinrichs and Lucey 2002; Hinrichs et al. 1999; Moroz et al. 2000; Schade and Wäsch 1999) confirmed the systematic temperature variations in olivine spectra reported by Singer and Roush. These temperature trends were used by Lucey et al. (2002) to interpret observed variations in spatially resolved spectra across the surface of 433 Eros and to confirm the presence of olivine.

Table 2. Observational details for meteorite spectra presented in this paper.

Meteorite class	Sample name	Composition	RELAB sample IB	Particle size	Spectral resolution	Incidence angle	Emergence angle
Pallasite	Thiel Mountain	Fa_{13}	MT-TJM-027	<75 μm	5 nm	30°	0°
Brachinite	EET 99402	Fa_{36}	TB-TJM-058	<125 μm	10 nm	30°	0°
R chondrite	Rumuruti	Fa_{39}	MT-TJM-013	<155 μm	10 nm	30°	0°

Although Lucey et al. (1998) compared low-temperature spectra of olivine with A-asteroid spectra, they only had low-temperature data for magnesian olivine. Attempts to extrapolate trends to more ferroan olivine were made, but were of limited value in the absence of data. Furthermore, their analysis was based on examination of the overall 1 μm absorption feature in olivine, and not the more detailed compositional information available from analysis of the three individual absorption bands. This was likely due to the quality of the then-available asteroid data from the 52-color survey (Bell et al. 1988). Thus, the conclusion that four A-asteroids are magnesian, and therefore related to pallasites (Lucey et al. 1998), needs to be re-examined.

In order to address the behavior of individual olivine absorption bands, Sunshine et al. (2000) examined the Hinrichs et al. (1999) spectra of olivine as a function of temperature using the MGM. From a theoretical perspective, thermal vibrations should broaden the width of crystal field absorptions, and if the cell size within the crystal structure also changes, can alter the position of absorption (Burns 1970, 1993). In certain structures, some absorptions are thermally coupled, which could also alter their relative strength as temperatures change (e.g., Burns 1974). MGM-based compositional inferences, including olivine composition, are dependent on the relative strength of absorptions (Sunshine and Pieters 1998). As temperature decreases, the spectra of forsteritic olivine exhibited negligible changes in the band positions, decreases in band widths for all three absorptions (with the greatest change in the central absorption), and significant changes in relative strengths as predicted by crystal field theory (Burns 1974, 1993). As indicated in Fig. 6, the changes in relative band strength between the M1 and M2 absorption bands as a function of temperature mimic the compositional variations in M1 versus M2 band strength (Fig. 3d). These variations are systematic and thus readily quantifiable. These systematic changes in band relative strength and width as a function of temperature can be incorporated as specific constraints in MGM models. The constraints need not be rigid, but, as with previous constraints on the widths and relative strengths in olivine absorptions at room temperature (Sunshine and Pieters 1998), can be included into the MGM with uncertainties.

Recently, in unpublished work, Sunshine et al. have similarly analyzed data from Hinrichs on the compositional variability of fayalite (from Rockport, Massachusetts, USA, Fa_{99}). As with magnesian olivine, spectra of ferroan olivine change systematically with temperature. Results for relative band strength of the M1 and M2 absorptions are shown in Fig. 6. While no data for intermediate olivine compositions have been measured, it is reasonable to expect similar trends in relative absorption band strengths with temperature. A temperature trend for intermediate composition (~Fa_{40}) olivine is linearly interpolated, as shown in Fig. 6. It is clear from these data, that a spectrum of a magnesian olivine at 175 K will have relative band strengths, and thus an overall shape, that is very similar to those in the spectrum of intermediate composition olivine at 250 K, a strong indication of the importance of temperature in interpreting olivine spectra.

These results call into question even recent conclusions on the composition of Main Belt olivine-rich asteroids (e.g., Lucey et al. 1998; Reddy et al. 2005; Sunshine et al. 1998; Sunshine and Pieters 1998). It is now clear that proper identifications of olivine composition need to simultaneously evaluate temperature and composition. However, this task is not as complex as it may seem, in that the approximate temperatures of asteroids are constrained by their heliocentric distances and albedos. Once temperature is determined, composition is then the only remaining variable.

TELESCOPIC SPECTRA OF ASTEROIDS

In this work, we examine spectra of eight olivine-dominated asteroids collected as part of an ongoing survey of silicate-rich asteroids using SpeX. These asteroids, the specific dates, and conditions of their observations are presented in Table 3. The data were reduced to relative reflectance following the procedure presented in Sunshine et al. (2004). Typical range in errors in relative reflectance based on Poisson statistics propagated through the data reduction process for both star and asteroid observations are 0.1–2% (excluding wavelengths with telluric absorptions). Spectra obtained on different nights differ in slope by 0–2%, but show no variation in absorption features above the noise. As such, spectra from different observations were combined into a single average spectrum by determining the error-weighted mean reflectance value at each spectral channel. This average near-infrared spectrum was then scaled and combined with visible data from the SMASS and SMASSII asteroid surveys (Bus and Binzel 2002b; Xu et al. 1995), using a scaling factor derived from the overlapping channels (0.82–0.92 μm) shared between the visible and near-infrared spectra. Based on the average heliocentric distance of the

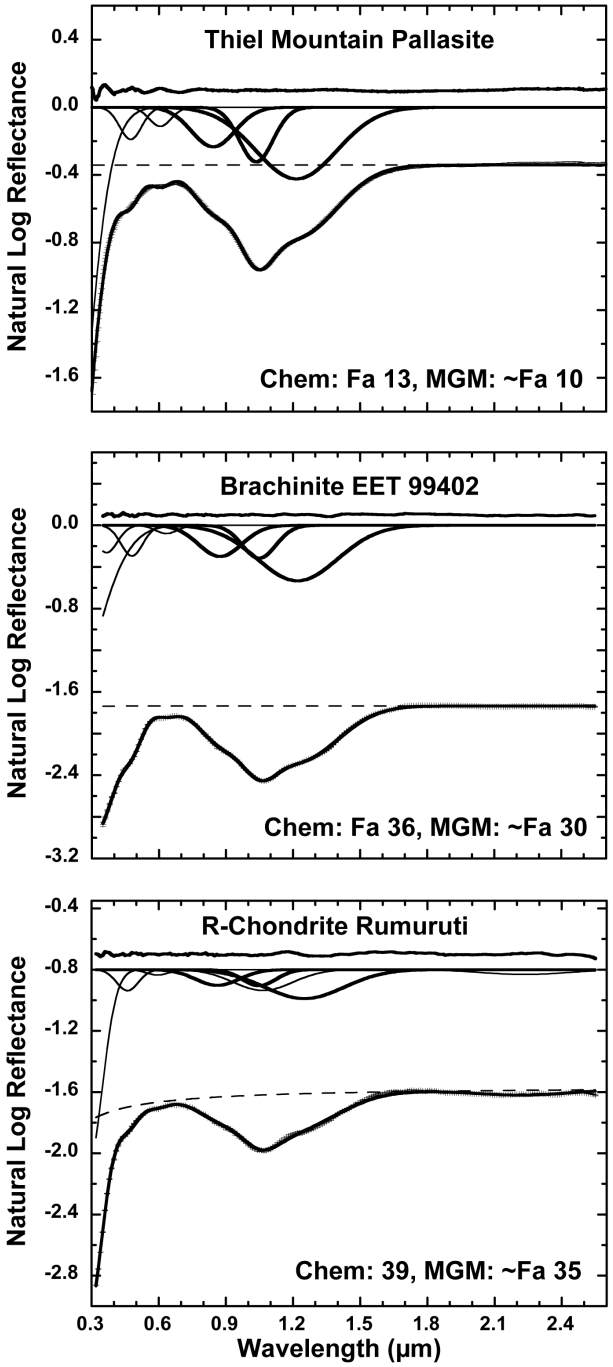

Fig. 5. MGM fits of olivine-rich meteorites. Compositions inferred from the MGM model agree very well with known compositions. Lines as in Fig. 3, with the characteristic olivine electronic transition absorptions in bold. Minor absorptions also occur at shorter wavelengths. Note that the Rumuruti spectrum includes a minor pyroxene phase with absorptions at 1 and 2 μm.

SpeX observations and typical values for model parameters, the average surface temperature for each asteroid was estimated (see Table 3) using the standard thermal model (Lebofsky and Spencer 1989).

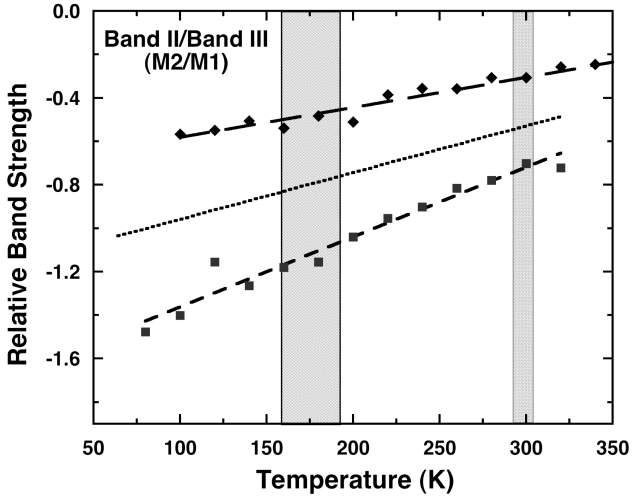

Fig. 6. Variations in relative band strengths of the M2 and M1 absorptions in olivine spectra as a function of temperature. Compare to compositional trend at room temperature (Fig. 3d). Temperature trends are plotted for measurements of magnesian (squares = Fa_{11}) and ferroan (diamonds = Fa_{99}) olivines. A trend for intermediate olivine compositions is linearly interpolated (dotted line) between the two measured trends. Approximate temperature regimes are indicated for Main Belt asteroids (~160–190 K) and laboratory and near-Earth objects (~300 K).

Of the eight SpeX spectra, only two, 354 Eleonora and 289 Nenetta include little to no absorptions in the 2 μm region, indicating they contain at most minor amounts of pyroxene. A third asteroid, 1951 Lick from de Leon et al. (2004), also lacks detectable 2 μm absorptions. The remaining spectra have detectable 2 μm absorptions, which based on visual analyses suggests on the order of 5–10% coexisting pyroxene (e.g., Cloutis et al. 1986). In future efforts, these spectra will be analyzed more rigorously to confirm this interpretation.

RESULTS

Spectral matching (i.e., visible comparisons) suggests that 1951 Lick and 289 Nenetta are very similar (see Fig. 7). Taken at face value, this would imply that they have similar compositions. While the spectra of 1951 Lick and 289 Nenetta are comparable, it is critical to note that they are from different parts of the asteroid population and thus have very different temperatures. As a near-Earth asteroid, 1951 Lick has a surface temperature near 250 K, while 289 Nenetta is in the Main Belt and has a surface temperature near 170 K.

Visual comparisons with olivine spectra at different temperatures are constructive. For example as suggested by Lucey et al. (1998), Fig. 8a compares continuum-removed and normalized spectra of two Main Belt asteroids 298 Nenetta and 354 Eleonora to the spectra of magnesian (Fa_{11}) olivine at 170 and 300 K. While the spectrum of 354 Eleonora of agrees well with the 170 K magnesian olivine,

Table 3. Observational details for asteroid spectra presented in this paper.[a]

Asteroid	Spectral range[b, c]	UT date	Exposure (sec)	Mean airmass	Precipit. water (mm)[d]	Helio. dist. (AU)	Phase angle (deg)	V magnitude	Mean temperature (K)[e]
246 Asporina	Vis	07-Jan-1994	360	1.33		2.92	19.6	14.1	185
	Vis	18-Apr-1996	540	1.14		2.48	8.0	12.1	
	Vis	19-Apr-1996	540	1.12		2.48	8.0	12.1	
	NIR	28-Mar-2001	1200	1.36	1.9	2.41	24.0	13.6	
	NIR	10-Apr-2005	1080	1.14	1.0	2.44	16.5	12.5	
	NIR	26-Apr-2005	1080	1.16	0.8	2.44	12.5	12.2	
289 Nenetta	Vis	13-Apr-1997	1350	1.06		3.22	17.4	15.2	190
	NIR	04-Sep-2000	1200	1.02	7.1	2.29	23.5	13.5	
	NIR	29-Jan-2001	1200	1.04	0.7	2.46	23.6	14.3	
354 Eleonora	Vis	27-Oct-1995	240	1.16		2.53	22.9	11.2	170
	Vis	22-Feb-1997	180	1.28		2.72	21.2	11.5	
	NIR	15-Apr-2002	960	1.11	1.1	2.91	19.9	11.5	
446 Aeternitas	Vis	06-Jan-1994	600	1.01		3.07	4.7	13.4	180
	Vis	07-Jan-1994	360	1.00		3.07	4.6	13.4	
	Vis	23-Feb-1994	1200	1.00		3.10	15.0	14.1	
	NIR	14-Aug-2001	840	1.40	1.4	2.44	9.2	12.3	
	NIR	12-Jan-2003	960	1.04	1.1	2.97	10.9	13.6	`
863 Benkoela	Vis	17-Jan-1997	900	1.03		3.22	1.9	13.5	160
	NIR	12-Jan-2003	1200	1.02	1.3	3.18	7.7	13.9	
984 Gretia	Vis	25-May-1997	900	1.80		2.51	23.5	13.8	190
	Vis	27-May-1997	900	1.77		2.50	23.4	13.7	
	NIR	16-Sep-2002	960	1.19	3.4	2.26	11.9	12.1	
	NIR	29-Sep-2002	1080	1.02	1.6	2.26	7.3	11.9	
2501 Lohja	Vis	30-Nov-1996	1800	1.08		2.87	12.0	16.6	190
	NIR	12-Jan-2002	1920	1.04	5.7	2.39	17.8	15.9	
3819 Robinson	Vis	20-Jan-1997	1800	1.00		2.71	6.9	16.2	180
	NIR	26-Jul-2004	2880	1.45	2.1	2.63	12.3	16.3	

[a]Eight SpeX spectra are presented here. An additional olivine-dominated object, 1951 Lick, with a temperature of ~250 K, is also analyzed using the spectrum of de León et al. (2004).

[b]Visible CCD spectra cover 0.44–0.92 μm and were taken with MDM Observatory 2.4 m Hiltner Telescope (Bus and Binzel 2002b).

[c]Near-infrared SpeX spectra cover 0.82–2.49 μm and were taken with 3.0 m NASA IRTF on Mauna Kea.

[d]Amount of precipitable water above Mauna Kea was determined from fits to telluric water bands in the SpeX data using the ATRAN model (Lord 1992).

[e]Approximate mean temperature calculated at average of observed heliocentric distances using the standard thermal model (Lebofsky and Spencer 1989). Standard values of emissivity = 0.9, phase angle = 0°, beaming parameter = 0.8, albedo = 0.3, and a slope parameter = 0.15, are assumed to derive these temperature estimates.

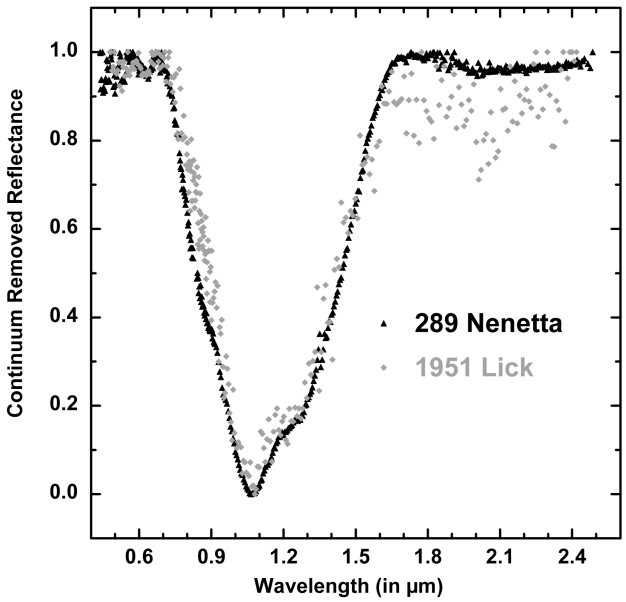

Fig. 7. Continuum removed and normalized spectra of 1951 Lick (de León et al. 2004) and 289 Nenetta. Visually the spectra of 1951 Lick and 289 Nenetta compare very favorably. However, because of differences in their surface temperatures (~250 K versus ~170 K), they must have different compositions.

the spectrum 289 Nenetta is inconsistent with magnesian olivine throughout the temperature range, and is therefore likely to be more ferroan.

We used the MGM to provide a more quantitative analysis of the A-asteroid spectra. Our approach is to first determine temperature and then evaluate composition. For each of the four olivine-dominated asteroids, various constrained MGM models were tested. Using a temperature appropriate for each object (175 K or 250 K), the relative band strengths between the M1 and M2 bands are constrained to values associated with magnesian, ferroan, or intermediate olivine compositions based on the data in Fig. 6. In addition, as in previous analyses (Sunshine and Pieters 1998) the band centers are initially set to be consistent with the assumed composition (see Fig. 3) and set to co-vary. Thus, for each asteroid three different compositional models are tested with a goal of determining which of these three broad compositional categories is most consistent with the measured spectrum. If the resulting band centers are broadly consistent with the compositional used to set constraints on the relative band strengths, the fit is deemed reliable. However, if, for example, a model with ferroan relative band strengths results in band centers that imply a magnesian composition, it is internally inconsistent and therefore considered unrealistic.

Results for each of the three compositional models at 250 K for 1951 Lick and at 175 K for 289 Nenetta, 354 Eleonora, and 246 Asporina are given in Table 4. For comparison, olivine compositions resulting from unconstrained MGM models are also tabulated. Based on the consistency criterion, this modeling implies that 1951 Lick is indeed magnesian (~Fa_{20}) as suggested by de León et al. (2004), as is the Main Belt asteroid 354 Eleonora (~Fa_{10}). However, 246 Asporina and 289 Nenetta are more ferroan with intermediate olivine compositions of ~Fa_{40}. The best model fits to 354 Eleonora and 289 Nenetta are shown in Figs. 8b and 8c, respectively.

The remaining five olivine-rich asteroids presented here (446 Aeternitas, 863 Benkoela, 984 Gretia, 2501 Lohja, and 3819 Robinson) appear to have ~5–10% co-existing pyroxene. Melt models presented earlier indicate that the presence of these amounts of pyroxene is consistent with lesser degrees of partial melting, ~45% for ordinary chondrites and ~<15% for R chondrites (Figs. 1 and 2). In addition, our modeling indicates that melts of ordinary chondrites will result in residuals that can include small amounts of low-calcium pyroxene, while residues of the more oxidized R chondrites contain high-calcium pyroxene. Reliable modeling of olivine-pyroxene mixtures is not trivial (Sunshine 1995), must take into account temperature effects, and therefore is beyond the scope of this paper. However, simple qualitative spectral matching (Fig. 9) suggests that the olivine in these asteroids (all of which are in the Main Belt and thus at low temperature) is most consistent with a magnesian olivine composition. Despite minor variations in pyroxene band position with temperature (Hinrichs and Lucey 2002; Roush and Singer 1987), the position of the 2 μm pyroxene bands suggests the remaining five olivine spectra include low-calcium pyroxene (Adams 1974; see Fig. 9). Thus, we preliminary conclude that this objects originate from ordinary chondritic sources. However, this conclusion must be verified in the future with more rigorous MGM modeling of spectra which include combinations of both pyroxene and olivine (Sunshine 1995).

DISCUSSION

Consistency tests of MGM models using temperatures appropriate for each asteroid have provided constraints on the composition of olivine on the surfaces of A-asteroids. Similar analyses of meteorite spectra that successfully predict the known olivine composition strongly argue that these results are reliable. In addition, melt models allow us to use the type (high- or low-calcium) of co-existing pyroxene as secondary control on petrologic origin of olivine-dominated surfaces.

Many of the asteroids analyzed here are magnesian. The only known petrologic pathway that produces magnesian olivine-dominated lithologies is from residues of high degrees of partial melting of chondrites with subsequent melt removal (e.g., mantle formation). For magnesian composition olivine-dominated asteroids, and likely many others that include <20% low-calcium pyroxene (from ~40% melting),

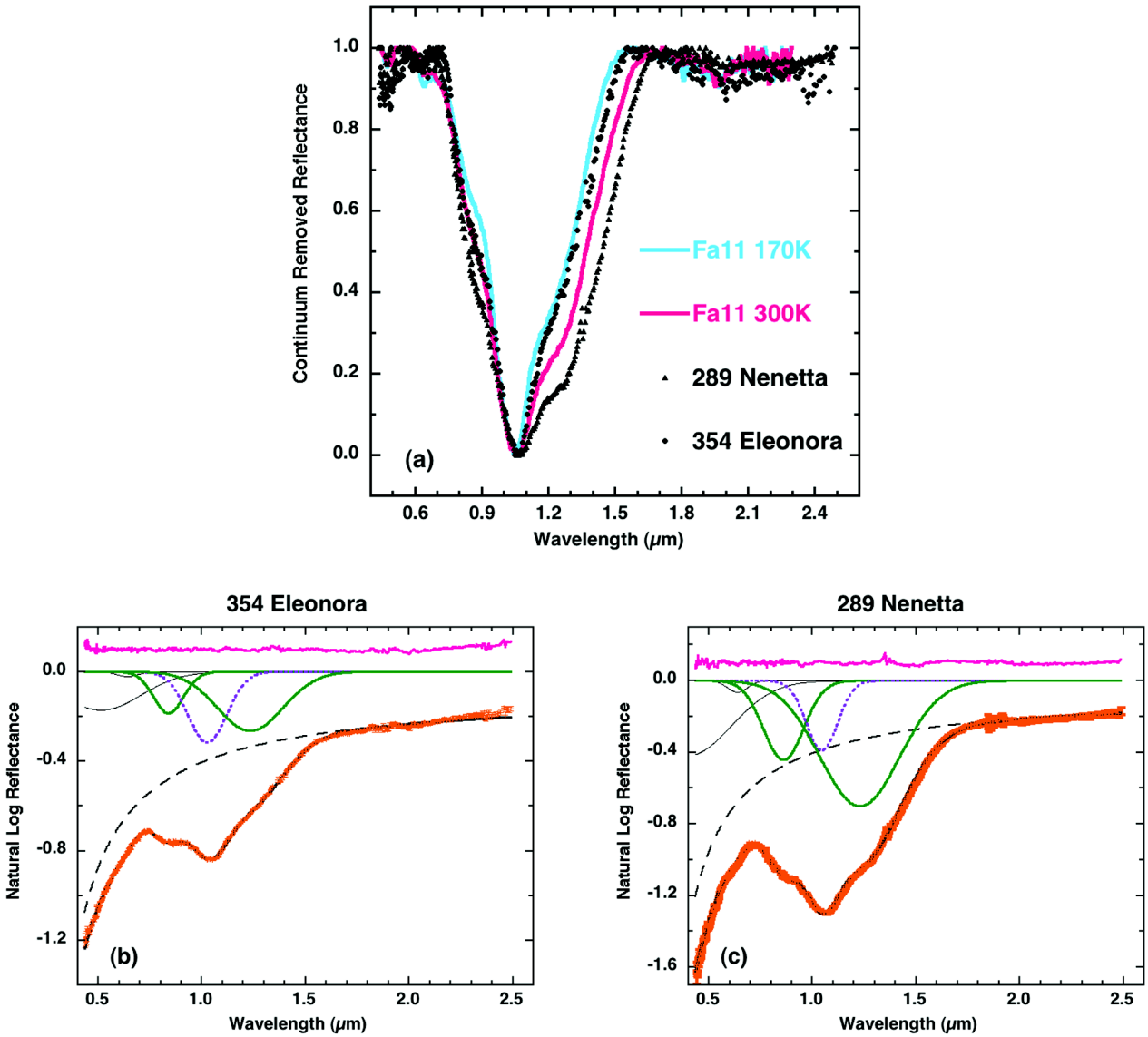

Fig. 8. Spectra of 289 Nenetta and 354 Eleonora. a) Continuum removed and normalized data compared to MgO-rich olivine at room temperature (300 K) and at temperatures near those found in the Main Belt (~170 K). The spectrum of 289 Nenetta is clearly inconsistent with MgO-rich olivine. MGM models of (b) 354 Eleonora and (c) 289 Nenetta (as in Fig. 3). Note the differences in relative band strengths of the M1 (solid green) versus M2 (dotted purple) absorption bands. Minor residuals in the 2 µm region suggest negligible pyroxene content in these spectra.

this is the likely origin. Thus, the canonical view of mantle formation for the origin of A-asteroids and analogies to pallasite (and pyroxene pallasite) meteorites are reasonable.

However, moderately ferroan composition olivine-dominated asteroids clearly require a different origin. Melting models confirm that olivine with composition >Fa_{20} cannot be produced from the melting and segregation of ordinary chondrites. Melting and segregation processes always produce more magnesian residues than the starting composition. Furthermore, while partial melts are more iron-rich, they also are enriched in plagioclase and pyroxene (see Sunshine et al. 2004).

To produce ferroan olivine surfaces, the starting materials must already be FeO-rich. In R chondrites, the olivine is more ferroan due to oxidation processes. Even small amounts of partial melting of R chondritic sources will still produce moderately ferroan olivine residues, as has been suggested as possible petrologic history of the brachinite meteorites (Nehru et al. 1996). However, significant melting, even of R-chondrite-like sources, results in more magnesian olivine residues. An alternative history for brachinites, and analogous moderately ferroan olivine-dominated asteroids, is that an oxidation event occurred during melting that converts Fe-metal to FeO (Mittlefehldt et al. 2003).

Table 4. Olivine compositions derived from MGM modeling of olivine-rich asteroids.

Asteroid name	MGM[a] 175 K	MGM 250 K	Fa_{10} 175 K	Fa_{10} 250 K	Fa_{50} 175 K	Fa_{50} 250 K	Fa_{90} 175 K	Fa_{90} 250 K
1951 Lick	*–20*[b]	09	n/a[c]	**21**[d]	n/a	*09*	n/a	*–04*
289 Nenetta	29	23	*38*	n/a	**40**	n/a	*52*	n/a
246 Asporina	31	21	*46*	n/a	**37**	n/a	*25*	n/a
354 Eleonora	10	09	**08**	n/a	*01*	n/a	*39*	n/a

[a]Unconstrained MGM model results. Other models test compositional solutions at a given temperature as explain in the text.
[b]Inferred compositions that are inconsistent with model assumptions are in italics.
[c]n/a are temperatures which are not applicable for the asteroid.
[d]Compositions that are fully consistent with model assumptions are in bold.

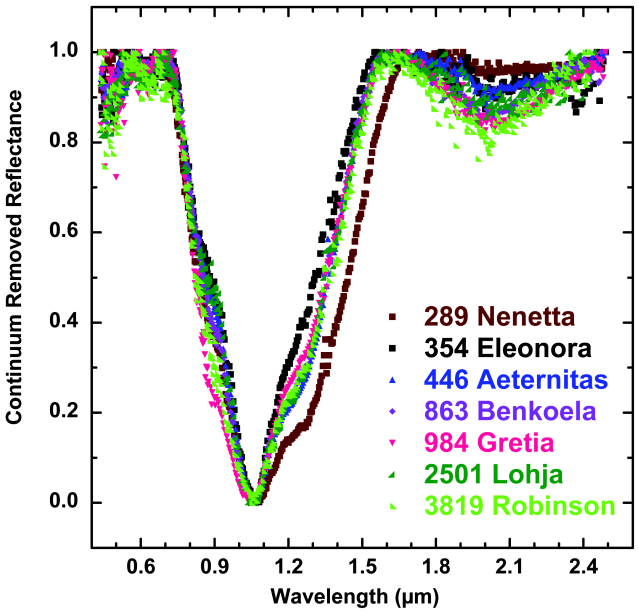

Fig. 9. Continuum removed and normalized spectra of five additional olivine-dominated Main Belt asteroids compared to 289 Nenetta and 354 Eleonora. While these spectra clearly include pyroxene absorptions near 2 μm, visual comparisons suggests that the olivine absorptions are more consistent with those in 354 Eleonora, and thus are more likely to be MgO-rich. In addition, the position of the pyroxene absorptions (<2.2 μm) implies a low-calcium pyroxene. Together this suggests that these asteroids are residuals from high degrees of melting of ordinary chondritic sources and thus likely are mantle samples as represented by pallasites.

CONCLUSIONS

Based on the meteorite record, we expect the asteroid population to include olivine-dominated surfaces with intermediate olivine compositions as occurs in brachinites and R chondrites. This expectation is consistent with the observed variability in the spectra of the nine olivine-dominated asteroids examined here. However, heliocentric distance, and thus surface temperature, has a significant effect on the spectra of olivine-rich asteroids that occur in both the Main Belt and the near-Earth populations. We have shown that spectrally composition and temperature interact in a complex way and must be simultaneously taken into account in order to infer olivine composition accurately.

Melting models indicate that the composition and abundance of olivine systematically co-vary and are therefore excellent petrologic indicators. Our analyses show that most of the olivine-dominated asteroids are magnesian and thus likely sampled mantles differentiated from ordinary chondrite sources. However, other olivine-rich asteroids are found to be more ferroan. Melting models show that partial melting cannot produce olivine-rich residues that are more ferroan than the chondrite precursor from which they formed. Thus, even moderately ferroan olivine must have non-ordinary chondrite origins, and therefore likely originate from oxidized R chondrite or melts thereof.

Of the nine olivine-dominated asteroid spectra examined to date, seven are magnesian, while two (289 Nenetta and 246 Asporina) are more ferroan. This proportion of magnesian to ferroan olivine-dominate asteroids reflects variations in nebular composition within the asteroid belt and is consistent with the meteoritic record in which R chondrites and brachinites are rare relative to pallasites.

Finally, as with the olivine-dominated surfaces analyzed here, temperature effects specifically need to be taken into account when examining the spectra of any lithologies that have a significant amount of olivine. This is particularly true for spectra of complex combinations of olivine and pyroxenes (e.g., ordinary chondrite-like bodies), where temperature alone will cause the spectra of Main Belt bodies to differ from laboratory spectra of meteorites. Thus, as with olivine-dominated lithologies, simple matching of meteorite and telescopic spectra is unlikely to correctly identify potential Main Belt parent bodies for ordinary chondrites.

Acknowledgments–Support for this research from NASA's Planetary Geology and Geophysics Program (NNX06AH69H to JMS), NSF (AST-0307688 to SJB), NASA's Cosmochemistry Program (NAG5-13464 to TJM and CMC), and the Becker Endowment to the Smithsonian Institution is greatly appreciated. All meteorite spectra were collected at Brown University's Keck/NASA Reflectance Experiment Laboratory (RELAB), a multi-user facility supported by NASA (NAG5-13609). Detailed comments and constructive suggestion for improvements by T. Roush and an anonymous reviewer are greatly appreciated.

Editorial Handling—Dr. Beth Ellen Clark

REFERENCES

Asimow P. D. and Ghiorso M. S. 1998. Algorithmic modifications extending melts to calculate subsolidus phase relations. *American Mineralogist* 83:1127–1132.

Bell J. F., Davis D. R., Hartmann W. K. and Gaffey M. J. 1989. Asteroids: The big picture. In *Asteroids II*, edited by Binzel R. P., Gehrels T., and Matthews M. S. Tucson, Arizona: The University of Arizona Press. pp. 921–945.

Bell J. F., Gaffey M. J., and Hawke B. R. 1984a. Spectroscopic identification of probable pallasite parent bodies (abstract). *Meteoritics* 19:187–188.

Bell J. F., Hawke B. R., Singer R. B., and Gaffey M. J. 1984b. The olivine asteroids: Discovery, mineralogy, and relationship to meteorites (abstract). 15th Lunar and Planetary Science Conference. pp. 48–49.

Bell J. F., Owensby P. D., Hawke B. R., and Gaffey M. J. 1988. The 52-color asteroid survey: Final results and interpretation (abstract). 19th Lunar and Planetary Science Conference. p. 57.

Boesenberg J. S., Davis A. M., Prinz M., Weisberg M. K., Clayton R. N., and Mayeda T. K. 2000. The pyroxene pallasites, Vermillion and Yamato-8451: Not quite a couple. *Meteoritics & Planetary Science* 35:757–769.

Brearley A. J. and Jones R. H. 1998. Chondritic meteorites. *Planetary materials*, edited by Papike J. J. Washington, D.C.: Mineralogic Society of America. pp. 3-1–3-398.

Burbine T. H. and Binzel R. P. 2002. Small Main Belt asteroid spectroscopic survey in the near-infrared. *Icarus* 159:468–499.

Burbine T. H., McCoy T. J., Jarosewich E., and Sunshine J. M. 2003. Deriving asteroid mineralogies from reflectance spectra: Implications for the MUSES-C target asteroid. *Antarctic Meteorite Research* 16:185–195.

Burns R. G. 1970. *Mineralogical applications of crystal field theory.* New York: Cambridge University Press. 224 p.

Burns R. G. 1974. The polarized spectra of iron in silicates: Olivine a discussion of neglected contributions from Fe^{2+} ions in M(1) sites. *American Mineralogist* 59:625–629.

Burns R. G. 1993. *Mineralogical applications of crystal field theory.* New York: Cambridge University Press. 551 p.

Bus S. J. and Binzel R. P. 2002a. Phase II of the small Main Belt asteroid spectroscopic survey: A feature-based taxonomy. *Icarus* 158:146–177.

Bus S. J. and Binzel R. P. 2002b. Phase II of the small Main Belt asteroid spectroscopic survey: The observations. *Icarus* 158: 106–145.

Chapman C. R. 1986. Implications of the inferred compositions of asteroids for their collisional evolution. *Memorie della Societa Astronomica Italiana* 57:103–114.

Cloutis E. A., Gaffey M. J., Jackowski T. L., and Reed R. L. 1986. Calibrations of phase abundance, composition, and particle size distributions for olivine-orthopyroxene mixtures from reflectance spectra. *Journal of Geophysical Research* 91:11,641–11,653.

Clark B. E., Hapke B., Pieters C., and Britt D. 2003. Asteroid space weathering and regolith evolution. In *Asteroids III*, edited by Bottke W. F., Jr., Cellino A., Paolicchi P., and Binzel R. P. Tucson, Arizona: The University of Arizona Press. pp. 585–599.

Cloutis E. A., Gaffey M. J., and Smith D. G. W. 1990. Metal silicate mixtures: Spectral properties and applications to asteroid taxonomy. *Journal of Geophysical Research* 95:8323–8338.

Cruikshank D. P. and Hartmann W. K. 1984. The meteorite-asteroid connection: Two olivine-rich asteroids. *Science* 223:281–283.

Gaffey M. J. 1998. Using nickel features in the spectra of olivine-dominated a- and S(I)-type asteroids to determine the oxidation state of the solar nebula. 29th Lunar and Planetary Science Conference (abstract). p. 1370.

Gaffey M. J., Bell J. F., Brown R. H., Burbine T. H., Piatek J. L., Reed K. L., and Chaky D. A. 1993. Mineralogical variations within the S-type asteroid class. *Icarus* 106:573–602.

Ghiorso M. S. and Sack R. O. 1995. Chemical mass transfer in magmatic processes IV. A revised and internally consistent thermodynamic model for the interpolation and extrapolation of liquid-solid equilibria in magmatic systems at elevated temperatures and pressures. *Contributions to Mineralogy and Petrology* 119:197–212.

Gomes C. B. and Keil K. 1980. Brazilian stone meteorites. NASA STI/Recon Technical Report A 82, 22886.

Hinrichs J. L. and Lucey P. G. 2002. Temperature-dependent near-infrared spectral properties of minerals, meteorites and lunar soil. *Icarus* 155:169–180.

Hinrichs J. L., Lucey P. G., Meibom A., and Krot A. N. 1999. Temperature dependent near-infrared spectra of olivine and H5 ordinary chondrites (abstract #1505). 30th Lunar and Planetary Science Conference. CD-ROM.

Hiroi T. and Sasaki S. 2001. Importance of space weathering simulation products in compositional modeling of asteroids: 349 Dembowska and 446 Asternitas as examples. *Meteoritics & Planetary Science* 36:1587–1596.

Jarosewich E. 1990. Chemical analyses of meteorites—A compilation of stony and iron meteorite analyses. *Meteoritics* 25: 323–337.

King T. V. V. and Ridley W. I. 1987. Relation of the spectroscopic reflectance of olivine to mineral chemistry and some remote sensing implications. *Journal of Geophysical Research* 92: 11,457–11,469.

Lebofsky L. A. and Spencer J. R. 1989. Radiometry and a thermal modeling of asteroids. In *Asteroids II*, edited by Binzel R. P., Gehrels T., and Matthews M. S. Tucson, Arizona: The University of Arizona Press. pp. 128–147.

de León J., Duffard R., Licandro J., and Lazzaro D. 2004. Mineralogical characterization of A-type asteroid. 1951. *Astronomy and Astrophysics* 422:L59–L62.

Lucey P. G., Hinrichs J., Kelly M., Wellnitz D., Izenberg N., Murchie S., Robinson M., Clark B. E., and Bell J. F. 2002. Detection of temperature-dependent spectral variation on the asteroid Eros and new evidence for the presence of an olivine-rich silicate assemblage. *Icarus* 155:181–188.

Lucey P. G., Keil K., and Whitely R. 1998. The influence of temperature on the spectra of A-asteroids and implications for their silicate chemistry. *Journal of Geophysical Research* 103: 5865–5871.

Mason B. 1963. Olivine composition in chondrites. *Geochimica et Cosmochimica Acta* 27:1011–1023.

McCord T. M., Clark R. N., Hawke B. R., McFadden L. A., Owensby P. D., Pieters C. M., and Adams J. B. 1981. Moon: Near-infrared spectral reflectance: A first good look. *Journal of Geophysical Research* 86:10,883–10,892.

McCoy T. J., Mittlefehldt D. W., and Wilson L. Forthcoming. *Asteroid differentiation*. Tucson, Arizona: The University of Arizona Press.

McFadden L. A., Goldman N. J., Gaffey M. J., and Izenberg N. R. 2005. Evidence for partial melting in reflectance spectra of 433 Eros (abstract #1561). 36th Lunar and Planetary Science Conference. CD-ROM.

McSween H. Y., Jr., Bennett M. E. III, and Jarosewich E. 1991. The mineralogy of ordinary chondrites and implications for asteroid spectrophotometry. *Icarus* 90:107–116.

Mittlefehldt D. W., Bogard D. D., Berkley J. L., and Garrison D. H. 2003. Brachinites: Igneous rocks from a differentiated asteroid. *Meteoritics & Planetary Science* 38:1601–1625.

Moroz L., Schade U., and Wäsch R. 2000. Reflectance spectra of olivine-orthopyroxene-bearing assemblages at decreased temperatures: Implications for remote sensing of asteroids. *Icarus* 147:79–93.

Mustard J. F. 1992. Chemical analysis of actinolite from reflectance spectra. *American Mineralogist* 77:345–358.

Nehru C. E., Prinz M., Weisberg M. K., Ebihara M. E., and Clayton R. N. 1996. A new brachinite and petrogenesis of the group. 27th Lunar and Planetary Science Conference. pp. 943–944.

Pieters C. M., Fischer E. M., Rode O., and Basu A. 1993. Optical effects of space weathering: The role of the finest fraction. *Journal of Geophysical Research* 98:20,817–20,824.

Pieters C. A., Taylor L. A., Noble S. K., Keller L. P., Hapke B., Morris R. V., Allen C. C., McKay D. S., and Wentworth S. 2000. Space weathering on airless bodies: Resolving a mystery with lunar samples. *Meteoritics & Planetary Science* 35:1101–1107.

Pieters C. M. and Hiroi T. 2004. Relab User's Manual. http://www.planetary.brown.edu/relab/.

Rayner J. T., Toomey D. W., Onaka P. M., Denault A. J., Stahlberger W. E., Vacca W. D., and Cushing M. C. 2003. *Spex: A medium-resolution 0.8–5.5 micron spectrograph and imager for the NASA infrared telescope facility.* San Francisco: Astronomical Society of the Pacific. pp. 362–382.

Reddy V., Hardersen P. S., Gaffey M. J., and Abell P. A. 2005. Mineralogy and temperature-induced spectral investigations of A-type asteroids 246 Asporina and 446 Aeternitas (abstract #1375). 36th Lunar and Planetary Science Conference. CD-ROM.

Roush T. L. and Singer R. B. 1987. Possible temperature variation effects on the interpretation of spatially resolved reflectance observations of asteroid surfaces. *Icarus* 69:571–574.

Rubin A. E., Fegley B., and Brett R. 1988. Oxidation state in chondrites. In *Meteorites and the early solar system*, edited by Kerridge J. F. and Matthews M. S. Tucson, Arizona: The University of Arizona Press. pp. 488–511.

Schade U. and Wäsch R. 1999. Near-infrared reflectance spectra from bulk samples of the two SNC meteorites Zagami and Nakhla. *Meteoritics & Planetary Science* 34:417–424.

Schulze H., Bischoff A., Palme H., Spettel B., Dreibus G., and Otto J. 1994. Mineralogy and chemistry of Rumuruti: The first meteorite fall of the new R-chondrite group. *Meteoritics* 29:275–286.

Singer R. B. and Roush T. L. 1985. Effects of temperature on remotely sensed mineral absorption features. *Journal of Geophysical Research* 90:12,434–12,444.

Sunshine J. M. 1995. Towards a more sophisticated approach to compositional interpretation of silicate absorptions in asteroid spectra (abstract). 26th Lunar and Planetary Science Conference. pp. 1377–1378.

Sunshine J. M., Binzel R. P., Burbine T. H., and Bus S. J. 1998. Is asteroid 289 Nenetta compositionally analogous to the brachinite meteorites? (abstract #1430). 29th Lunar and Planetary Science Conference. CD-ROM.

Sunshine J. M., Bus S. J., Burbine T. H., and McCoy T. J. 2005. Tracing oxygen fugacity in asteroids and meteorites through olivine composition (abstract #1203). 36th Lunar and Planetary Science Conference. CD-ROM.

Sunshine J. M., Bus S. J., McCoy T. J., Burbine T. H., Corrigan C. M., and Binzel R. P. 2004. High-calcium pyroxene as an indicator of igneous differentiation in asteroids and meteorites. *Meteoritics & Planetary Science* 39:1343–1357.

Sunshine J. M., Hinrichs J. L., and Lucey P. G. 2000. Temperature dependence of individual absorptions bands in olivine: Implications for inferring compositions of asteroid surfaces from spectra (abstract #1605). 31st Lunar and Planetary Science Conference. CD-ROM.

Sunshine J. M. and Pieters C. M. 1993. Estimating modal abundances from the spectra of natural and laboratory pyroxene mixtures using the modified Gaussian model. *Journal of Geophysical Research* 98:9075–9087.

Sunshine J. M. and Pieters C. M. 1998. Determining the composition of olivine from reflectance spectroscopy. *Journal of Geophysical Research* 103:13,675–13,688.

Sunshine J. M., Pieters C. M., and Pratt S. F. 1990. Deconvolution of mineral absorption bands: An improved approach. *Journal of Geophysical Research* 95:6955–6966.

Tholen D. J. 1984. Asteroid taxonomy from cluster analysis of photometry. Ph.D. thesis, The University of Arizona, Tucson, Arizona, USA.

Ueda Y., Miyamoto M., Mikouchi T., and Hiroi T. 2003. Surface material analysis of the S-type asteroids: Removing the space weathering effect from reflectance spectrum (abstract #2078). 34th Lunar and Planetary Science Conference. CD-ROM.

Veeder G. J., Matson D. L., and Kowal C. 1982. Infrared (Jhk) photometry of asteroids (abstract). *Bulletin of the American Astronomical Society* 14:719.

Veeder G. J., Matson D. L., and Tedesco E. F. 1983. The R asteroids reconsidered. *Icarus* 55:177–180.

Wetherill G. W. and Chapman C. R. 1988. Asteroids and meteorites. In *Meteorites and the early solar system*, edited by Kerridge J. F. and Matthews M. S. Tucson, Arizona: The University of Arizona Press. pp. 35–67.

Xu S., Binzel B. P., Burbine T. H., and Bus S. J. 1995. Small Main Belt asteroid spectroscopic survey: Initial results. *Icarus* 115:1–35.